X-Ray Image Authentication Scheme Using SLT and Contourlet Transform for Modern Healthcare System

Vijay Krishna Pallaw

(School of Computing, Graphic Era Hill University, Dehradun, India
https://orcid.org/0000-0003-4819-4521, vijaykpallaw@gmail.com)

Kamred Udham Singh

(Department of Computer Science and Information Engineering, National Cheng Kung University, Taiwan,
School of Computing, Graphic Era Hill University, Dehradun, India
https://orcid.org/ 0000-0002-7201-6381, kamredudhamsingh@gmail.com)

Abstract: The network's convenience has created a copyright dilemma for some multimedia works. Nowadays, every healthcare system relies on digital medical images for diagnosis. These medical images are transmitted through communication channels, so there is a risk of tampering and copyright violation. A digital watermarking system can ensure and guarantee that tampering and copyright violation are prevented. This study presents a nonblind digital watermarking approach to X-ray medical images based on Contourlet transform (C.T.) and Slantlet Transform (SLT). Since the two-dimensional signals are represented flexibly by contourlet transforms, the contour plot can be used efficiently to represent curves and smooth contours. At the same time, the SLT has better time-localization & smoothness properties. The maximum energy of an image is conceived in the LL band if SLT transform are employed. Therefore, the LL band is used to entrench the watermark. The additive quantization method has been used to entrench the watermark. The efficiency of our scheme is assessed by different quality parameters and compared with several existing schemes. The results of the experiment show that the proposed scheme performs better and has the ability to resist several attacks.

1 Introduction

Nowadays, millions of users are sharing data on the World Wide Web. The most important concerns of these data are security, integrity, copyright & tamper protection, etc. [Li et al. 2015], [Zheng et al. 2015]. These concerns are also closely connected to multimedia images. To prevent the issues related to these concerns, there should be some standard solution. To protect the contents of images to be tampered with or to violate the copyright, digital watermarking could be a better solution. An imperceptible mark being inserted into the host image is the key idea behind digital watermarking [Thomas and Sucharitha 2022]. The ability of the watermark to resist several attacks can be categorized as robust or fragile. A robust watermark is resistant to specific attacks, whereas fragile ones do not resist and can be easily destroyed. Blind, non-blind, or semi-blind are three different types of watermarking techniques [Su et al. 2016],

[Singh et al., 2022(a)]. The original image is not mandatory to extract the watermark in blind watermarking. The original image may or may not be mandatory to extract the watermark in semiblind watermarking. Whereas the original image is mandatory for watermark extraction in nonblind watermarking systems [Narasimhulu and Prased 2011].

The digital image watermarking method is based on the media used, which are divided into the spatial domain and the frequency domain. In the spatial domain the watermark images are directly entrenched in the image. The watermarking in the frequency domain is carried out through transforming the image into its frequency and then entrenching the watermark [Singh et al. 2018], [Singh and Singhal 2018]. The frequency domain embedding technique is more robust and has a high payload capacity. The usage of multimedia has affected various aspects of day-to-day life such as business, education, health care, etc. Various types of multimedia images are being used in the health care system, such as X-ray, MRI, mammography, CT-scan, ultrasound images, etc. [Sadreazami et al. 2014]. These images contain crucial data that must be protected from tampering that could lead to an incorrect diagnosis when transmitted over the network. Therefore, securing medical images is essential in the health care system. There are four major characteristics of medical image security: confidentiality, reliability, authenticity, and availability [Singh et al., 2022(b)]. To protect medical images from tampering, various research is available in the literature. In [Bi et al. 2010], Contourlet transform-based watermarking technique has been proposed. The improvement in the multiplicative watermarking system was presented in [Akhaee et al. 2010]. [Sadreazami et al. 2014] advises to entrench 1000 randomly generated watermark bits. In [Mohamad and Malcolm 2007], an algorithm to embed a watermark has been proposed based on contourlet transform. In [Niu et al. 2011], a watermarking technique has been derived that uses resisting geometric colour image watermarking. The basis of this technique was support vector regression and contourlet transform. Moreover, some of the watermarking systems are based on contourlet transform and matrix putrefaction as proposed in [Bhatnagar and Wu 2013], [Golea et al. 2010], [Naderahmadian and Hosseini-Khayat 2013], [Seddik et al. 2009], [Su et al. 2014].

On the basis of the above literature, a nonblind grayscale X-ray medical image watermarking system has been proposed in this paper. The fusion of contourlet transform and slantlet transform is the building block of this work to achieve the benefits of frequency domain. The SLT has been employed on low-frequency coefficients of contourlet transform to increase the robustness and good visibility of the watermarked images.

This paper is organised as follows: Section 2 examines the literature review and establishes the background for our work. In Section 3, the watermark entrenching and extraction algorithm are explained. The results are discussed and exhibited in Section 4. The conclusion is drawn in Section 5.

2   Related Work

This section establishes the foundation of our work. The frequency domain transformation is the common choice for all researchers who are working in watermarking. The frequency domain transforms the image into its frequency

coefficients and watermarks are entrenched into it. Wavelets are commonly practiced in frequency domain watermarking. Wavelets are able to represent image discontinuities in one dimension only. In contrast, the curvelet can efficiently represent discontinuities in two dimensions. The main characteristics of contourlet transform are multi-directionality and anisotropy. Moreover, the Slant let transform [Ivan, 1998], gives better localization and smoothness properties. It can control two zeros along with discrete time. It does not use filter banks to iterate, which results in better time localization. Therefore, we have chosen contourlet transform and slantlet transform for our algorithm.

There are few works available in the literature that use Contourlet transform for watermarking. In [Bi et al. 2010], a Contourlet and SVD based watermarking scheme was proposed on color images. An improved version of this scheme was proposed in [Akhaee et al. 2010], in which the 128 bits data was embedded into a grayscale image. In [Sadreazami et al. 2014], another version of this scheme was proposed as an improvement that can embed 1000 randomly generated watermark bits. A nonblind watermarking scheme was proposed in [Liang et al. 2008] that uses the blue channel of the host image. [Niu et al. 2011] proposition is based on support vector regression. It has the ability to resist geometric attacks.

Moreover, a blind watermarking scheme was proposed which modifies more than one singular value [Golea et al. 2010]. A QR decomposition-based watermarking scheme was proposed on a grayscale image. This method has low complexity in terms of computation and has good performance [Naderahmadian and Hosseini-Khayat 2013]. [Bhatnagar and Wu 2013] uses Hessenberg transform to entrench a watermark into the color image.

Moreover, [Jasni and Abdul 2006] reported a fragile watermarking to identify, tamper, and recover the image. It uses a chaotic algorithm and a key to entrench a watermark in the grayscale ultrasound image. An enhancement of this algorithm was proposed in [Jasni and Abdul 2007], in which the tamper detection rate has been increased. This algorithm distributes the watermark evenly, minimizes watermark distortion, and improves the quality of the image. A lossless watermarking algorithm was proposed in [Mohamad and Malcolm 2007], to recover the original image. This algorithm has a large payload and low distortion. A similar approach has been proposed in [Chiang et al. 2008].

In [Zhang and Sun 2019], a contourlet transform-based visual saliency watermarking technique was introduced. In this work, the low-pass subband coefficients are transformed into nonoverlapping blocks; the saliency values determine the quantization steps. A blind watermarking scheme was proposed in [Fan et al. 2019], which usages adaptive quantization. The mean of blocks decides the quantization step. In this scheme, the adaptive characteristics of blocks are decided to embed the strength of the watermark. A watermarking algorithm based fusion of contourlet transform and DCT was proposed in [Tian et al. 2020], in which the low pass frequency is partitioned into 8 x 8 nonoverlapping blocks. In [Senthilkumar and Periasamy 2020], a neuro-fuzzy based watermarking algorithm was proposed that uses neuro-fuzzy computation to entrench watermark bits into the green channel of the image. A watermarking system which uses frequency localization of contourlet transform based on SVD was introduced in [Najafi and Loukhaoukha 2019]. Another watermarking scheme was proposed by [Gong et al. 2021], which uses canny edge identification in the contourlet domain. The Canny edge recognition was performed on the coefficient of the U matrix

of SVD. The above literature motivated us to develop a watermarking system based on the fusion of contourlet transform and SLT transform.

2.1 Arnold Transform

The main purpose of Arnold transform (AT) is scrambling. It is to scramble the position of pixels in image processing to reduce the storage space [Sui and Gao 2013]. A matrix of M x M and coordinates are $C = \{(x,y)|x,y = 0,1,2,...M-1\}$. The AT can be expressed as follows:

$$\begin{pmatrix} x_n \\ y_n \end{pmatrix} = \begin{pmatrix} 1 & a \\ b & ab+1 \end{pmatrix} \begin{pmatrix} x_{n-1} \\ y_{n-1} \end{pmatrix} mod\ M$$

Here, x_n and y_n are the coordinates which are used to transform with respect to x_{n-1} and y_{n-1} after m number of iteration respectively, a and b are positive numbers, and M is the width and height of a square matrix. The IS iterative in nature, when (x, y) is transformed many times. It returns to into original form.

2.2 Contourlet Transform

The transform that usages multiscale filtering and works in the continuous domain was coined as contourlet transform. It is also known as second-generation curvelet transform since frequency partitioning replaces the Ridgelet transform. To represent the adaptiveness and a process to detect the edge, a contourlet transform is required. The Laplacian Pyramid (L.P.) is used to achieve multiscale decomposition. In L.P. decomposition, the original image with a low pass filter is generated at every level. To represent the smooth contour of the image, contourlet transform usages L.P. and directional filter bank as double filter bank structure. The directional filter bank is connected through L.P. and captured at the point of discontinuity [Cunha et al. 2006].Figure. 1 depicts four-level contourlet transform has been performed on X-ray grayscale image. In Figure 1 (b), the contourlet transform has been performed using two, four, eight, and sixteen directions. In this figure, larger coefficients are represented with white colour, whereas small ones are represented by black.
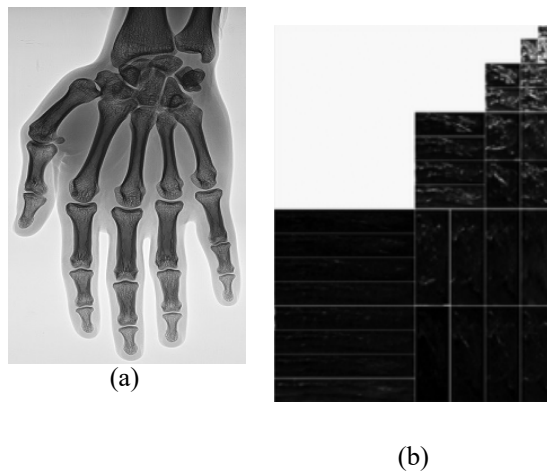

(a)

(b)

Figure 1: (a) X-ray, (b) contourlet transform on X-ray

2.3   Slantlet Transform

Slantlet transform [Ivan, 1998], gives better localization and smoothness properties. It has the ability to control two zeros along with discrete time. To iterate, it does not use filter banks which results in better time localization. A parallel structure is implemented as a solution of the SLT of the filter bank. The length of SLT filter is much smaller compared to discrete wavelets. To analyze the signals of filter of SLT on the scale of i, its length is directly proportional to 2^i.

SLT filter bank usages $g_i(n)$, $f_i(n)$, and $h_i(n)$ filters to construct their filter banks. The filter bank of SLT have twice the number of channels with respect to filter bank. $f_i(n)$ is an adjacent filter with the low pass filter $h_i(n)$. The downsampling is used for all filters by 2^L, and the rest of the filters are time reverse. The parameters ($a_{0,0}$, $a_{0,1}$, $a1,0$, and $a_{1,1}$) which are used to describe the filter $g_i(n)$ are as follows.

$$g_i(x) = \begin{cases} a_{0,0} + a_{0,1}n & for \; n = 0, \dots 2^i - 1 \\ a_{1,0} + a_{1,1}(n-2) & for \; n = 2^i, \dots 2^{i+1} - 1 \end{cases}$$

Eight parameters are used to describe the $f_i(n)$ and $h_i(n)$ filters.

$$f_i(x) = \begin{cases} b_{0,0} + b_{0,1}n & for \; n = 0, \dots 2^i - 1 \\ b_{1,0} + b_{1,1}(n-2) & for \; n = 2^i, \dots 2^{i+1} - 1 \end{cases}$$

$$h_i(x) = \begin{cases} c_{0,0} + c_{0,1}n & for \; n = 0, \dots 2^i - 1 \\ c_{1,0} + c_{1,1}(n-2) & for \; n = 2^i, \dots 2^{i+1} - 1 \end{cases}$$

3   Proposed Scheme

3.1   Watermark Embedding Process

In this section, the proposed watermark entrenching and extraction algorithms are described. The procedure to entrench the watermark is depicted in Figure 2. The Contourlet transform is employed on the host image, then SLT is performed.

The coefficient of low-frequency subband of the SLT is used to build the blocks of size 2 x 2. The watermark image is scrambled using Arnold scrambling, then the image is converted into a single-dimensional vector. The watermark bits are quantized using the additive quantization technique. Afterwards, the inverse SLT is employed, and the inverse contourlet transform is employed to get the watermarked image. The algorithm to entrench the watermark is explained as follows.

Step 1: Employ contourlet transform on host image (H) → H_c.
Step 2: Apply Slantlet transform to hc obtained in the previous step.
Step 3: Convert the low-frequency subband obtained in the previous step (L.L.) into the
       block of a size of 2 x 2.
Step 4: Apply Arnold scrambling on the watermark image (W) → W_a and convert it
       into a one-dimensional vector.
Step 5: Watermark bits are quantized into the block obtained in step 3.

Step 6: Inverse Slantlet transform and inverse contourlet transform are employed to get the watermarked image.
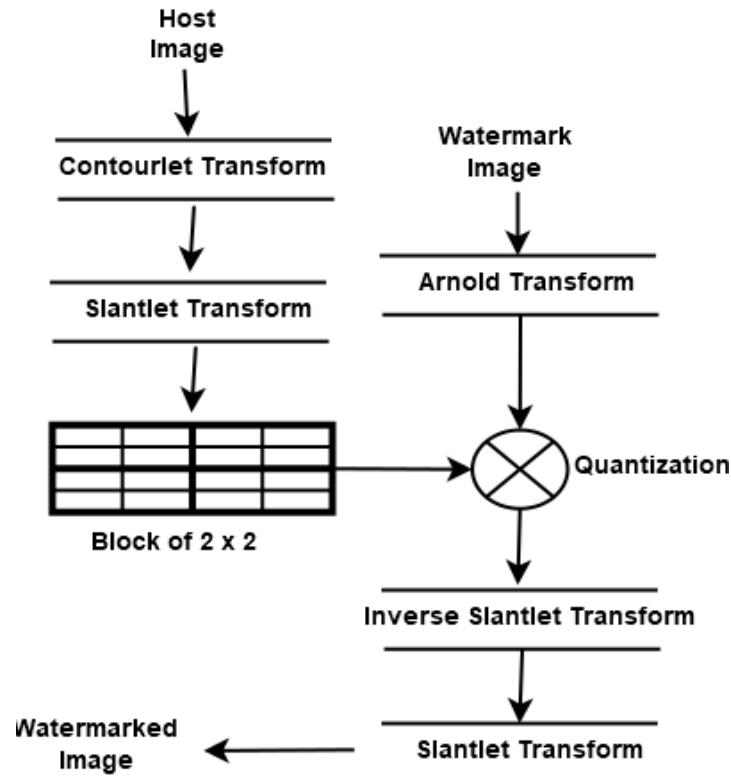

Figure 2: Block diagram for the watermark embedding process

3.2 Watermark Extraction Process

In Figure 3, the watermark extraction process has been depicted. In the first step of the extraction process, the contourlet transform is performed on both images (i.e., original and watermarked images). Then SLT transform is performed. In the dequantization process, the coefficients are subtracted from each other to get watermark bits. These watermark bits are rescrambled using Arnold transform. Finally, the watermark is extracted. The algorithm to extract the watermark is explained as follows.

Step 1: Employ Contourlet transform on the original (O) and watermarked image

(W ').

Step 2: Apply Slantlet transform to both images.

Step 3: Convert the low-frequency subband obtained in the previous step (L.L.) into the

block of the size of 2 x 2. This step is also performed on both images.

Step 4: Compare the coefficients of both images to obtain watermark bits.

Step 5: Apply Arnold scrambling on the watermark bits to get the watermark.
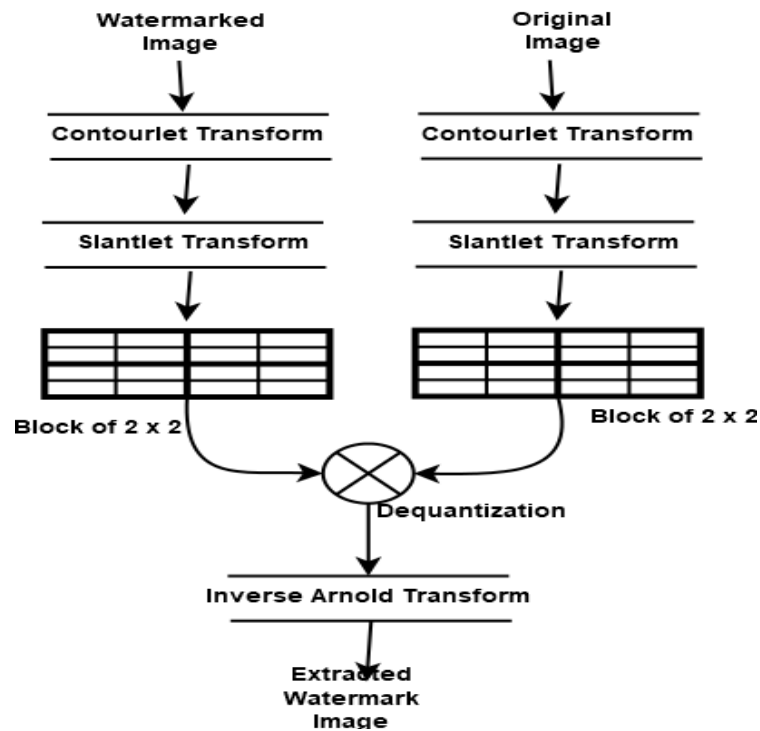

Figure 3: Block diagram for extraction process

4   Results and Discussion

In this work, we have anticipated a fusion of contourlet transform and SLT based watermarking system on grayscale X-ray images. Figure 4 shows the grayscale X-ray images and a bitmap image, which have been used in our experiment. The information related to the patient has been intentionally removed for privacy and security reasons.

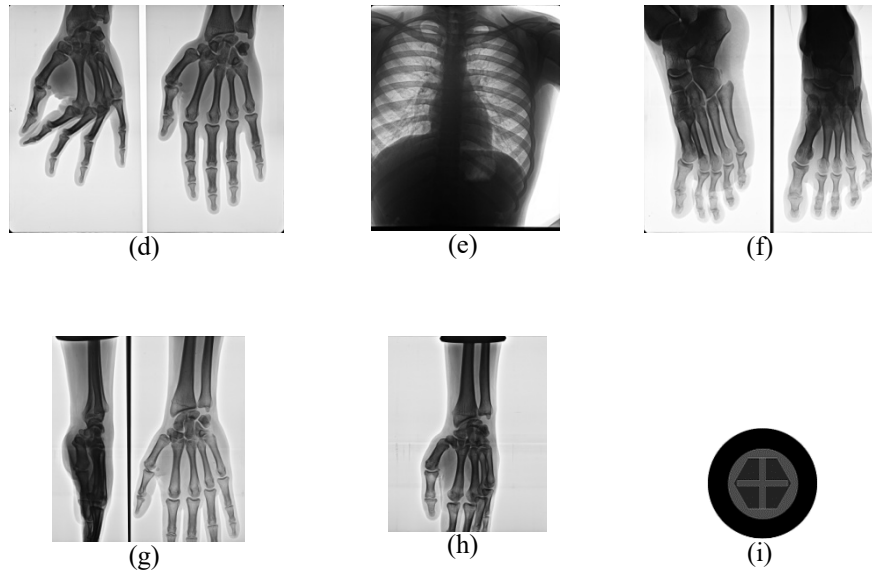(a)   (b)   (c)

(d) (e) (f)

(g) (h) (i)
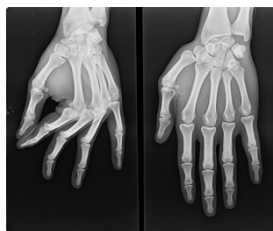
Figure 4: X-ray images used in the experiment (a) – (h) and watermark image (i)

A number of quality parameters have been used to assess the effectiveness of the scheme. To assess the original image's distortion after applying the watermark's entrenching procedure, the peak signal-to--to-noise ratio (PSNR) has been used. The equation to calculate PSNR is as follows:

$$PSNR_{dB} = 10\log_{10}\left[M*N\frac{\max^2(i,j)}{\sum i,j[l(i,j)-J(i,j)]^2}\right]$$

Furthermore, any change in the number of pixels with respect to the integration process (NPCR) compared to the original image are calculated as follows:

$$NPCR = \sum_{i=1}^{M}\sum_{j=1}^{N}\frac{D(i,j)}{T}*100$$

To compare the image's visual perception with the original image as well as the discrepancy between them is shown as follows [Singh et al., 2022(c)]:

$$SSIM\,(x,y) = \frac{(2\mu_x\mu_y + C_1)(2\delta_{xy} + C_2)}{(\mu_x^2 + \mu_y^2 + C_1)(\delta_x^2 + \delta_y^2 + C_2)}$$

Various types of X-ray images have been used in our experiment, but we are only showing two images in this experiment due to some limitations. In table 1, the PSNR, SSIM, and N.C. have been shown after entrenching a watermark into the host images.

The PSNR of images 1 & 2 are 52.5412 & 52.5319, respectively. The high value of the watermarked image exhibits good visual quality of the image. The high PSNR of the results shows that the performance of our work is quite good and acceptable.

Image	PSNR	SSIM	NC
(a)	52.5412	0.9777	0.9908
(b)	52.5319	0.9818	0.9908
(c)	51.8895	0.9716	0.9911
(d)	52.0012	0.9805	0.9908
(e)	51.9891	0.9799	0.9908
(f)	51.8879	0.9748	0.9908
(g)	52.5126	0.9786	0.9908
(h)	52.5123	0.9803	0.9908

Table 1: PSNR, SSIM, and N.C. after embedding the watermark

In Table 2, the PSNR & SSIM values have been shown after imposing different types of attacks. The high PSNR value after different image processing attacks shows that the anticipated technique is more robust. The high-intensity attacks that have been applied to the watermarked scheme would change the PSNR of the watermarked image. The SSIM of the extracted watermark is approximately 1, which shows that the extraction algorithm can identify the watermark under high-intensity attacks.

Attack	PSNR	SSIM	EXTRACTED WATERMARK
No attack	52.5412	0.9908	
Speckle Noise	39.4578	0.8980	
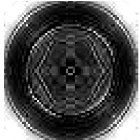
Salt & Pepper noise	40.0912	0.8921	
Median filter	40.1451	0.8811	
JPEG 2000	38.5545	0.8052	
JPEG	40.9987	0.7702	
Sharpening attack	40.2156	0.8642	
Motion blur	38.8812	0.7996	
Scaling	40.9652	0.8132	

Table 2: PSNR & SSIM after various attacks

Table 3 exhibits the comparison of our work with other similar schemes. In our case, we have achieved high PSNR and SSIM compared to other related work. In the work,

the PSNR is 52.5412, whereas the different schemes shown in Table 3 below are much smaller, ranging from 35dB to 45dB. Therefore, we can conclude that our algorithm performs much better than other similar schemes. We have also compared our results using structural similarity index measures. Here, we have observed that SSIM between the original and watermarked images is high.

	[Thomas and Sucharitha 2022]	[Su 2016]	[Golea et al. 2010]	[Su et al. 2014]	[Narasimhulu and Prased 2011]	Proposed work
PSNR	45.31	48.3033	38.4358	35.3521	44.7899	52.5412
SSIM	0.9954	0.9955	0.9935	0.9589	0.9714	0.9801

Table 3: Comparison of PSNR of proposed work with other related work

We have also evaluated our scheme on the basis of various image processing attacks on existing algorithms and found that the extraction process of the watermark is performing much better than theirs.

Attack	[Golea et al. 2010]	[Su et al. 2014]	[Narasimhulu and Prased 2011]	[Su 2016]	Proposed work
JPEG	0.6009	0.7028	0.7084	0.7109	0.7702
JPEG 2000	0.9750	0.9971	0.9996	0.9998	0.8052
Salt and pepper noise	0.5827	0.8114	0.8817	0.99121	0.8921
Median filtering	0.4779	0.7137	0.7866	0.7962	0.8811
Scaling	0.4881	0.8121	0.8026	0.8713	0.8132

Table 4: Comparison of SSIM of the extracted watermark with other related work after different attacks

5   Conclusions

A nonblind grayscale X-ray medical image watermarking technique has been anticipated in this work. The proposed scheme is a fusion of contourlet transform and Slantlet transform. The watermark is scrambled using Arnold transform to ensure the security and robustness of the scheme. The proposed scheme uses the low-frequency band of contourlet transform, and the L.L. subband was used to entrench the watermark. The results shown in our experiment outperform in contrast to other techniques in terms of visual quality and resistance to several types of attacks. However, our work is limited to grayscale images only. In the near future, we will try to apply our algorithm to color images and video as well.

References

[Akhaee et al. 2010] Akhaee M. A., Sahraeian S. M. E., Marvasti F.: "Contourlet-based image watermarking using optimum detector in a noisy environment"; IEEE Trans Image Process 19, 4 (2010), 967–980.

[Bhatnagar and Wu 2013] Bhatnagar, G., Wu, Q. M. J.: "Biometrics inspired watermarking based on a fractional dual tree complex wavelet transform"; Future Generation Computer Systems, 29, 1 (2013), 182–195.

[Bi et al. 2010] Bi H., Li X., Zhang Y., Xu Y.: "A blind robust watermarking scheme based on C.T. and SVD"; In: Proceedings of 2010 I.E. 10th International Conference on Signal Processing (ICSP), (2010), 881–884.

[Cunha et al. 2006] Cunha, A. L., Zhou, J., Do, M. N.: "The nonsubsampled contourlet transform: theory, design, and applications"; IEEE transactions on image processing, 15, 10 (2006), 3089–3101.

[Fan et al. 2019] Fan, D., Wang Y., Chunwei Z.: "A blind watermarking algorithm based on adaptive quantization in Contourlet domain"; Multimedia Tools and Application, 78, 7 (2019), 8981–8995.

[Golea et al. 2010] Golea N. E. H., Seghir R., Benzid R.: "A bind RGB color image watermarking based on singular value decomposition"; In: 2010 IEEE/ACS International Conference on Computer Systems and Applications (AICCSA), (2010), 1–5.

[Gong et al. 2021] Gong, L. H., Tian, C., Zou, W. P. et al.: "Robust and imperceptible watermarking scheme based on Canny edge detection and SVD in the contourlet domain"; Multimed Tools Applications, 80 (2021), 439–461.

[Ivan, 1998] Ivan W. S.: "The slantlet transform"; IEEE transactions on signal processing, 47, 5 (1999), 1304–1313.

[Jasni and Abdul 2006] Jasni M. Z., Abdul R .M. F.: "Medical image watermarking with tamper detection and recovery"; Engineering in Medicine and Biology Society, EMBS'06. 28th Annual International Conference of theIEEE, (2006), 3270–3273.

[Jasni and Abdul 2007] Jasni M. Z., Abdul R. M. F.: "Evaluation of medical image watermarking with tamper detectionand recovery (aw-tdr)"; In 2007 29th Annual International Conference of the IEEE Engineering in Medicine and Biology Society, (2007), 5661–5664.

[Chiang et al. 2008] Chiang, K., Chang, K., Chang, R., Yen H.: "Tamper detection andrestoring system for medical images using wavelet-based reversible data embedding"; Journal of DigitalImaging, 21,1 (2008), 77–90.

[Sui and Gao 2013] Sui, L., Gao B.: "Color image encryption based on gyrator transform and Arnold transform"; Optics and Laser Technology, 48, (2013), 530–538.

[Li et al. 2015] Li, J., Li, X., Yang, B., & Sun, X.: "Segmentation-based image copy-move forgery detection scheme"; IEEE Trans Inf Forensics Secur, 10, 3 (2015), 507–518.

[Liang et al. 2008] Liang, D., Yin, B., Yu, M., Li, X., & Wang N. D.: "An algorithm for color image digital watermarking using the non sub sampled Contourlet transform"; Acta Optica Sinica, 28, 8 (2008), 1469–1474.

[Mohamad and Malcolm 2007] Mohamad, Z., Malcolm, C.: "Reversible region of non-interest (roni) watermarking for authentication of dicom images"; International Journal of Computer Science and Network Security, 7, 9 (2007), 19–28.

[Naderahmadian and Hosseini-Khayat 2013] Naderahmadian, Y., Hosseini-Khayat, S.: "Fast and robust watermarking in still images based on Q.R. decomposition"; Multimedia Tools Applications, 72, 3 (2013), 2597–2618.

[Najafi and Loukhaoukha 2019] Najafi, E., K. Loukhaoukha.: "Hybrid secure and robust image watermarking scheme based on SVD and sharp frequency localized contourlet transform"; Journal of information security and applications, 44 (2019),144–156.

[Narasimhulu and Prased 2011] Narasimhulu, C. V., Prased K. S.: "A new SVD hybrid color image watermarking for copyright protectionusing Contourlet transform"; International journal of computer applications, 20, 8 (2011), 18–27.

[Niu et al. 2011] Niu, P. P., Wang, X. Y., Yang, Y. P., Lu, M. Y.: "A novel color image watermarking scheme in nonsampled contourlet-domain"; Expert System Appllications, 38, 3 (2011), 2081–2098.

[Sadreazami et al. 2014] Sadreazami, H., Ahmad, M. O., Swamy, M. N. S.: "A study of multiplicative watermark detection in the contourlet domain using alpha-stable distributions"; IEEE Transaction on Image Processing, 23, 10 (2014), 4348–4360.

[Seddik et al. 2009] Seddik, H., Sayadi, M., Fnaiech, F., Cheriet, M.: "Image watermarking based on the Hessenberg transform"; International Journal of Image and Graphics, 9, 3 (2009), 411–433.

[Senthilkumar and Periasamy 2020] Senthilkumar, M., and Periasamy P. S.: "Contourlet transform and adaptive neuro-fuzzy strategy–based color image watermarking"; Measurement and Control, 53, 4 (2020), 287–295.

[Singh et al. 2022(a)] Singh, K. U., Hsieh, S. Y., Swarup, C., Singh, T.: "Authentication of NIfTI Neuroimages Using Lifting Wavelet Transform, Arnold Cat Map, Z-Transform, and Hessenberg Decomposition"; Traitement du Signal, 39, 1 (2022), 265–274.

[Singh et al. 2022(b)] Singh, K. U., Kumar, A., Singh, T., Ram, M.: "Image-based decision making for reliable and proper diagnosing in NIFTI format using watermarking"; Multimedia Tools and Applications, (2022), 1–27.

[Singh et al. 2022(c)] Singh, K. U., Abu-Hamatta, H. S., Kumar, A., Singhal, A., Rashid, M., Bashir, A. K.: "Secure watermarking scheme for color DICOM images in telemedicine applications"; Computers, Materials and Continua, 70, 2 (2022), 2525–2542.

[Singh et al. 2018] Singh, K. U., Singh, V. K., Singhal, A.: "Color image watermarking scheme based on QR factorization and DWT with compatibility analysis on different wavelet filters"; Journal of Advanced Research in Dynamical and Control Systems, 10, 06 (2018), 1796–1811.

[Singh and Singhal 2018] Singh, K. U., Singhal, A.: "Channelized noise augmentation to endorse DICOM medical image for diagnosing"; Journal of Advanced Research in Dynamical and Control Systems, 10, 06 (2018), 2228–2247.

[Su et al. 2014] Su, Q., Niu, Y., Zou, H., Zhao, Y, Yao, T.: "A blind double color image watermarking algorithm based on Q.R. decomposition"; Multimedia tools and applications, 72, 1 (2014), 987–1009.

[Su 2016] Su, Q.: "Novel blind color image watermarking technique using Hessenberg decomposition"; IET image processing, 10, 11(2016), 817–829.

[Thomas and Sucharitha 2022] Thomas, R., and Sucharitha, M.: "Contourlet and Gould Transforms for Hybrid Image Watermarking in RGB Color Images"; Intelligent Automation & Soft Computing, 33, 2 (2022), 879–889.

[Tian et al. 2020] Tian, C., Wen, R. H., Zou, W. P., Gong, L. H.: "Robust and blind watermarking algorithm based on DCT and SVD in the contourlet domain." Multimedia Tools and Applications, 79, 11 (2020), 7515–7541.

[Zhang and Sun 2019] Zhang, Y., Sun, Y.: "An image watermarking method based on visual saliency and contourlet transform"; Optik, 186 (2019), 379–389.

[Zheng et al. 2015] Zheng Y, Jeon, B., Xu, D., Wu, Q. M. J., Zhang, H.: "Image segmentation by generalized hierarchical fuzzy Cmeans algorithm"; Journal of Intelligent & Fuzzy Systems, 28, 2 (2015), 961–973.